ISSN No:-2456-2165 https://doi.org/10.38124/ijisrt/26jan461

Electromagnetically Realizable Super-Directive Hmimo Arrays for Near-Field 6G Communications

Uche Agwu[1*]; Matthew Ehikhamenle[2]

[1;2]Centre for Information & Telecommunication Engineering, University of Port Harcourt, Nigeria

Corresponding Author: Uche Agwu[1*]

[1][ORCID: 0009-0001-5325-2397]

Publication Date: 2026/01/16

Abstract: Super-directive holographic massive multiple-input multiple-output (HMIMO) antenna arrays are a key enabler for near-field beamforming, spatial focusing, and interference suppression in sixth-generation (6G) wireless systems. Although classical super-directive synthesis can, in principle, deliver extreme directivity, its physical realization is constrained by electromagnetic limits such as excessive reactive energy storage, bandwidth collapse, impedance mismatch, mutual coupling, and radiation-efficiency degradation. This paper presents an electromagnetic-aware design and validation framework for physically realizable near-field super-directive HMIMO arrays. The framework combines near-field array theory with fundamental bounds on directivity, quality factor (Q), sidelobe behavior, and realized gain, while explicitly enforcing practical constraints on excitation magnitudes, matching (S11), and efficiency. Full-wave electromagnetic simulations (CST Microwave Studio) are used to validate optimized planar HMIMO arrays across multiple aperture sizes. Results show that, when electromagnetic constraints are embedded in the design process, super-directive HMIMO arrays can generate highly focused near-field beams with stable impedance response and acceptable radiation efficiency, supporting practical 6G deployments in user-centric communications, integrated sensing and communication, localization, and wireless power transfer.

Keywords*: Super-Directive Antennas, Holographic Massive MIMO, Near-Field Beamforming, Electromagnetic Realizability, 6G Communications.*

How to Cite: Uche Agwu; Matthew Ehikhamenle (2026) Electromagnetically Realizable Super-Directive Hmimo Arrays for Near-Field 6G Communications. *International Journal of Innovative Science and Research Technology,* 11(1), 799-806. https://doi.org/10.38124/ijisrt/26jan461

I. INTRODUCTION

Sixth-generation (6G) wireless systems aim to unify communication, sensing, localization, and energy transfer within a single platform, demanding unprecedented spatial control of electromagnetic energy. Holographic massive multiple-input multiple-output (HMIMO) arrays, which approximate a continuous electromagnetic aperture through dense element packing, provide a natural pathway to near-field focusing where spherical wavefronts dominate. In this regime, spatial degrees of freedom increase, enabling distance-dependent beam focusing and spatial selectivity beyond far-field steering paradigms.

Super-directive arrays offer a theoretical mechanism to sharpen spatial focusing through carefully synthesized amplitude and phase excitations. However, the historical super-directivity paradox remains: pushing directivity beyond conventional aperture limits rapidly increases stored reactive energy, inflating Q, shrinking bandwidth, degrading efficiency, and destabilizing impedance. These challenges intensify in dense HMIMO arrays due to strong mutual coupling.

This paper consolidates and refines a thesis-derived study into a single journal-grade contribution focused on electromagnetically realizable near-field super-directive HMIMO arrays. The emphasis is not on abstract optimization alone, but on a design corridor bounded by electromagnetic law and validated through full-wave simulation.

II. THEORETICAL REVIEW

Near-field operation occurs when users lie within the Fresnel region, where spherical-wave propagation and distance-dependent phase variations are non-negligible. For a

ISSN No:-2456-2165 https://doi.org/10.38124/ijisrt/26jan461

planar HMIMO aperture, near-field focusing is achieved by synthesizing element excitations that produce constructive interference at a desired focal location and destructive interference elsewhere. Classical bounds (e.g., Harrington's directivity ceiling and Wheeler–Chu Q limits) show that extreme directivity is accompanied by rapidly growing reactive energy storage, high Q, and bandwidth collapse. Modern treatments emphasize that the relevant objective is not directivity alone, but realized gain under matching and efficiency constraints, particularly for dense apertures where coupling alters the effective impedance environment. Figure 1 illustrates that achievable gain is fundamentally limited by the electrical size of the radiating structure. It provides the theoretical motivation for why extreme super-directivity cannot be pursued without incurring severe electromagnetic penalties. This bound frames the realism of all subsequent HMIMO designs presented in the paper.

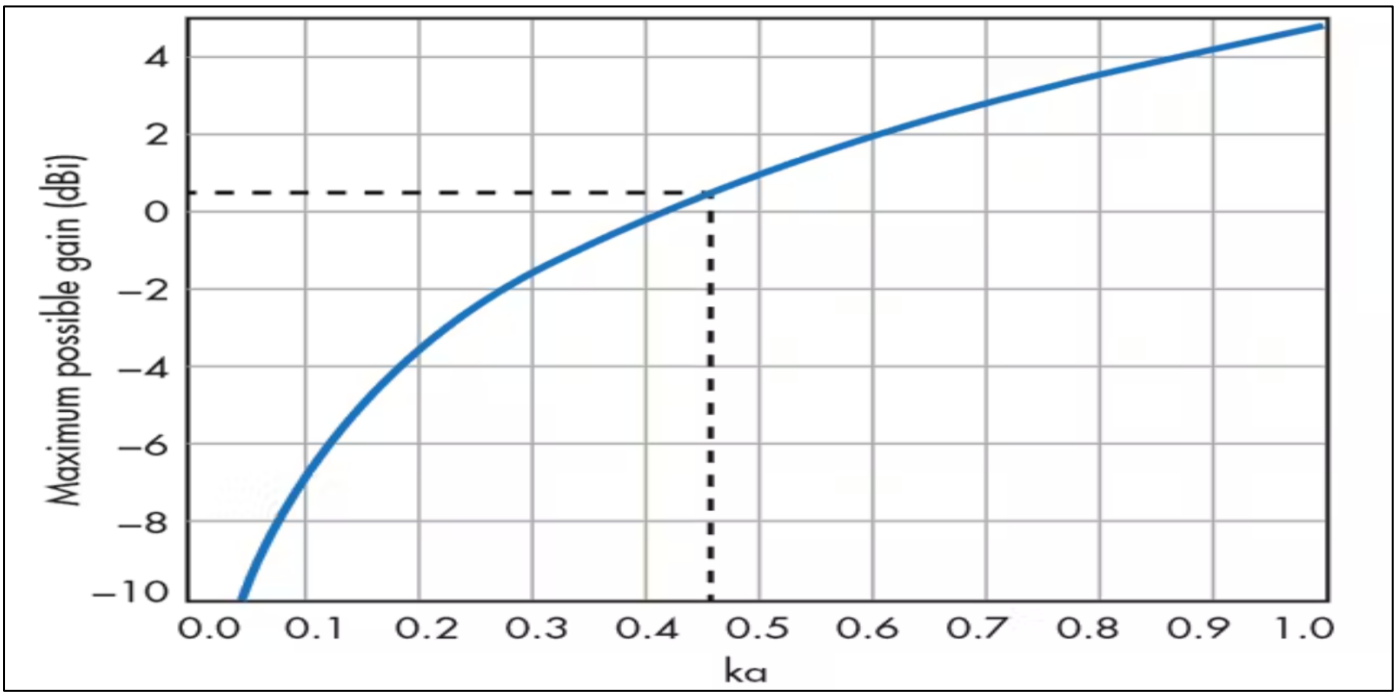

Fig 1 Harrington's Gain Versus Electrical Size (ka).

➢ *Adapted from Sharma and Nagarkoti (2017).*

Figure 2 shows that as electrical size decreases or as directivity is pushed beyond conventional limits, the quality factor increases rapidly, leading to narrow bandwidth and sensitivity to detuning. It directly supports the paper's argument that super-directivity must be constrained to remain physically realizable.

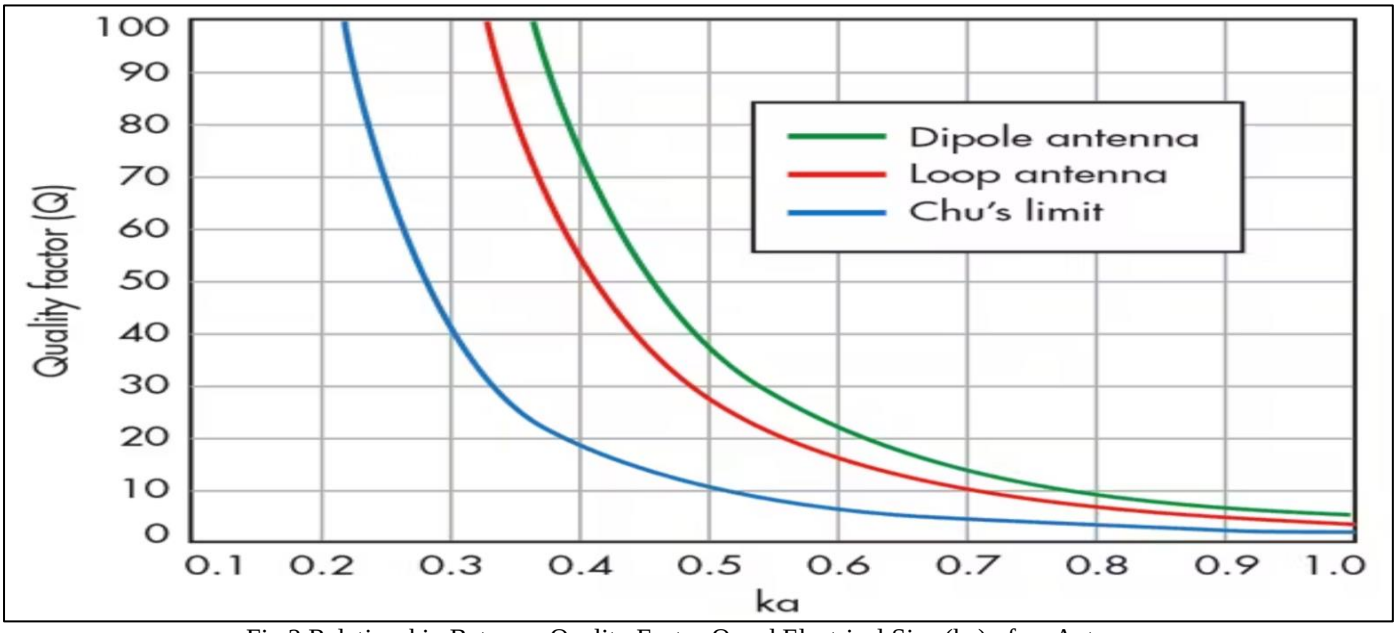

Fig 2 Relationship Between Quality Factor Q and Electrical Size (ka) of an Antenna.

ISSN No:-2456-2165 https://doi.org/10.38124/ijisrt/26jan461

Empirical studies on super-gain and super-directive arrays consistently report narrow operational bandwidth, strong sensitivity to tolerance and detuning, and realized-gain shortfalls relative to directivity predictions when losses and mismatch are included. In dense HMIMO surfaces, these effects are amplified by mutual coupling, necessitating full-wave modeling for credible feasibility assessment.

III. METHODOLOGY

The super-directive HMIMO array synthesis problem is formulated as a constrained multi-objective optimization problem. Consider a planar HMIMO array consisting of N radiating elements, each characterized by a complex excitation coefficient:

$$a_n = A_n e^{j\phi_n}, \quad n = 1, 2, \ldots, N$$

Where A_n and ϕ_n denote the excitation amplitude and phase of the nth antenna element, respectively.

Accordingly, the optimization design vector is expressed as:

$$\mathbf{X} = [A_1,\ \phi_1,\ A_2,\ \phi_2,\ \ldots,\ A_N,\ \phi_N]$$

For a focal point r_f in the Fresnel region, the electric field can be expressed as a coherent superposition of element contributions. A practical synthesis objective is to maximize |E(r_f)| while penalizing energy leakage outside the focal region and enforcing impedance and efficiency constraints.

To ensure electromagnetic realizability, constraints are imposed on input matching, radiation efficiency, sidelobe levels, and excitation magnitudes. This approach avoids converging to mathematically optimal yet physically unusable super-directive solutions characterized by extreme Q, unstable impedance, or severe efficiency collapse.

All candidate HMIMO arrays are validated using CST Microwave Studio. The simulation model includes realistic element structures, finite conductivity, dielectric losses, mutual coupling, and open boundary conditions. Array sizes spanning 2×2 to 20×20 elements are evaluated to assess scalability.

Figure 3 summarizes the end-to-end design process, from excitation synthesis and constraint enforcement to full-wave validation. It clarifies how electromagnetic constraints are embedded directly into the design loop, ensuring that optimized solutions remain physically meaningful.

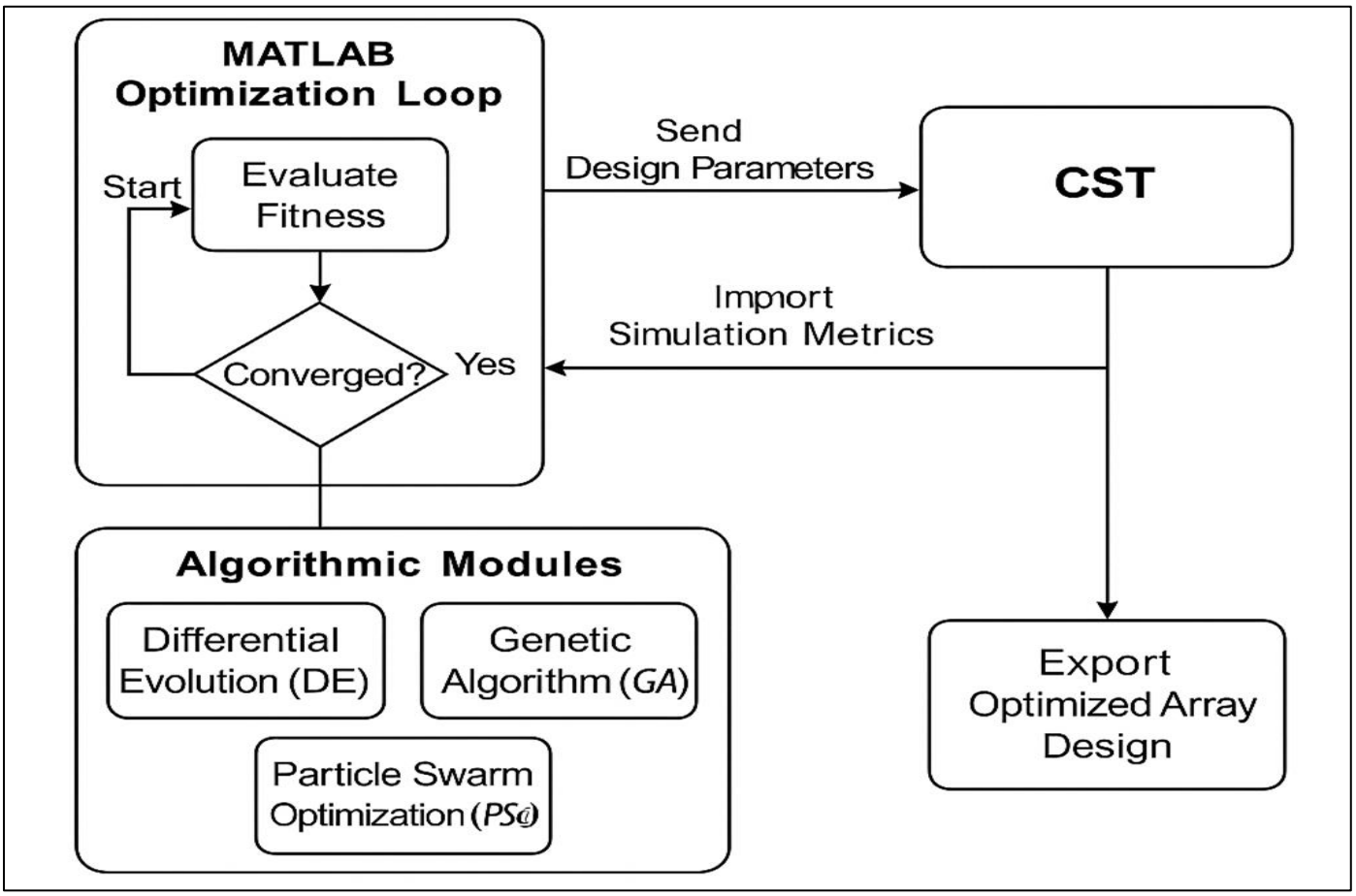

Fig 3 Overall Framework and Flow Architecture of the Optimization Method.

Figure 4 illustrates the planar HMIMO configuration, element arrangement, and aperture layout used throughout the simulations. It ensures reproducibility by clearly defining the geometry under which near-field focusing and super-directivity are evaluated.

ISSN No:-2456-2165 https://doi.org/10.38124/ijisrt/26jan461

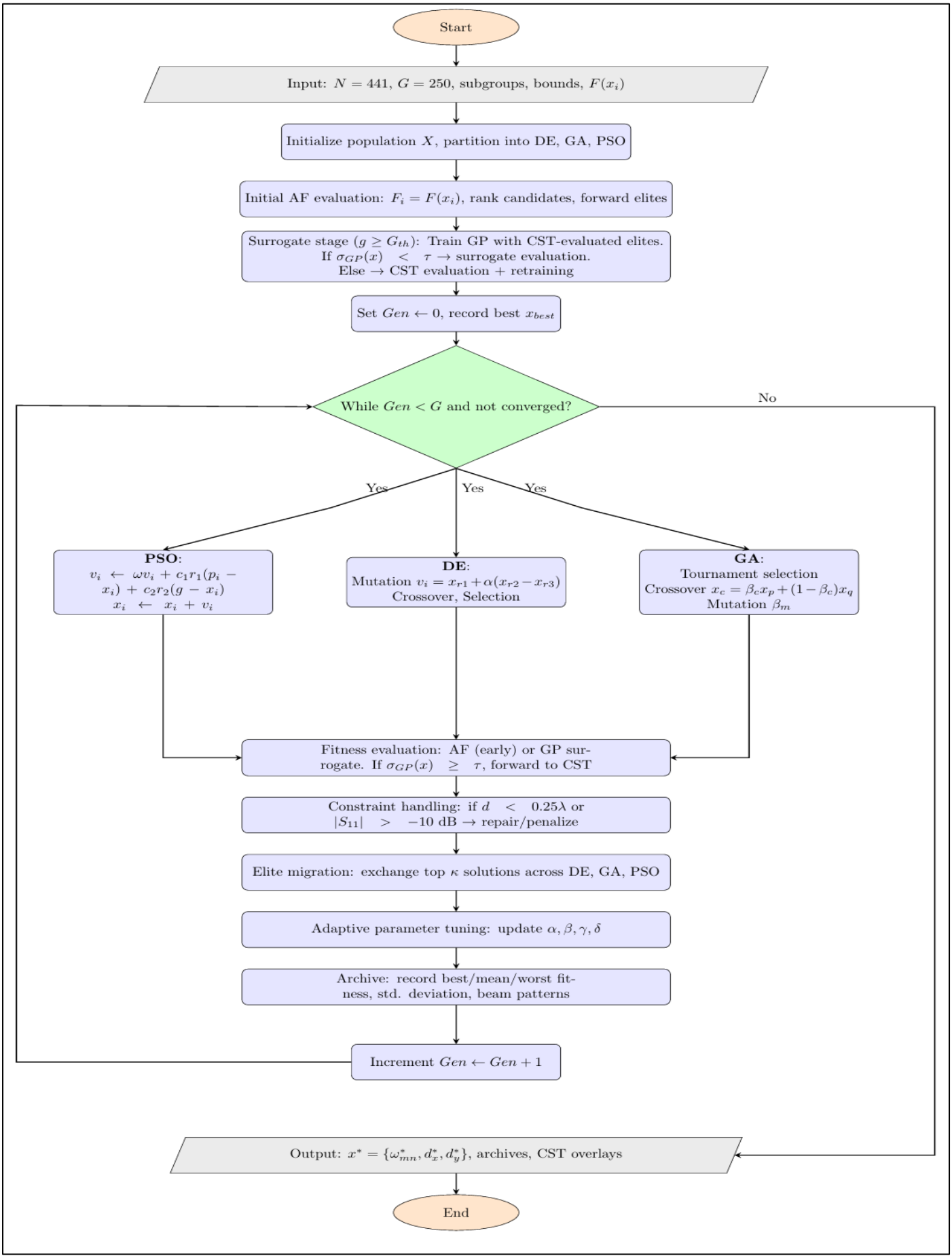

Fig 4 Planar HMIMO Array Geometry Used for Synthesis and Validation.

ISSN No:-2456-2165 https://doi.org/10.38124/ijisrt/26jan461

Table 1 summarizes CST-extracted metrics including realized gain, S11, HPBW, directivity, and sidelobe level across array sizes. It confirms that near-field super-directivity remains stable under full-wave conditions.

Table 1 CST Results for Evo-HMAA-Optimized Arrays

Array Size (M×N)	Elements	Realized Gain (dBi)	Return Loss (S_{11}, dB)	HPBW (°)	Directivity (dBi)	SLL (dB)
2×2	4	10.140	-18.750	63.12	16.026	-311.960
4×4	16	16.154	-18.556	29.90	22.043	-311.960
6×6	36	19.656	-17.654	19.89	25.561	-85.583
8×8	64	22.089	-19.960	12.96	28.004	-50.085
10×10	100	23.905	-18.127	10.80	29.701	-56.120
12×12	144	24.315	-18.195	9.25	31.115	-54.237
14×14	196	24.780	-21.217	7.92	32.211	-51.349
16×16	256	25.345	-19.202	6.75	33.289	-50.911
18×18	324	25.287	-19.142	6.45	34.182	-56.944
20×20	400	25.053	-19.023	5.12	34.940	-58.841

Table 2 presents MATLAB-based simulation results used during excitation synthesis. Comparison with Table 1 demonstrates strong agreement between numerical optimization and full-wave validation.

Table 2 MATLAB-Simulated Performance Metrics

Array Size (M×N)	Elements	Realized Gain (dBi)	Return Loss (S_{11}, dB)	HPBW (°)	Directivity (dBi)	SLL (dB)
2×2	4	10.140	-18.790	59.80	16.026	-310.960
4×4	16	16.154	-18.631	26.20	22.043	-310.960
6×6	36	19.672	-17.954	17.00	25.561	-86.783
8×8	64	22.114	-20.420	12.60	28.004	-51.085
10×10	100	23.810	-18.407	10.00	29.701	-56.120
12×12	144	25.220	-18.203	8.40	31.115	-54.237
14×14	196	26.320	-21.317	7.20	32.211	-50.349
16×16	256	27.400	-19.402	6.20	33.289	-51.111
18×18	324	28.290	-19.542	5.60	34.182	-56.044
20×20	400	29.050	-19.028	5.00	34.940	-58.941

IV. RESULTS AND DISCUSSION

The optimized super-directive HMIMO configurations produce enhanced directivity and improved sidelobe behavior relative to baseline excitation strategies, while maintaining stability under enforced electromagnetic constraints.

Figure 5 presents a three-dimensional radiation plot demonstrating strong spatial confinement and enhanced directivity relative to conventional excitation. It confirms that near-field super-directivity can be achieved while maintaining stable radiation behavior.

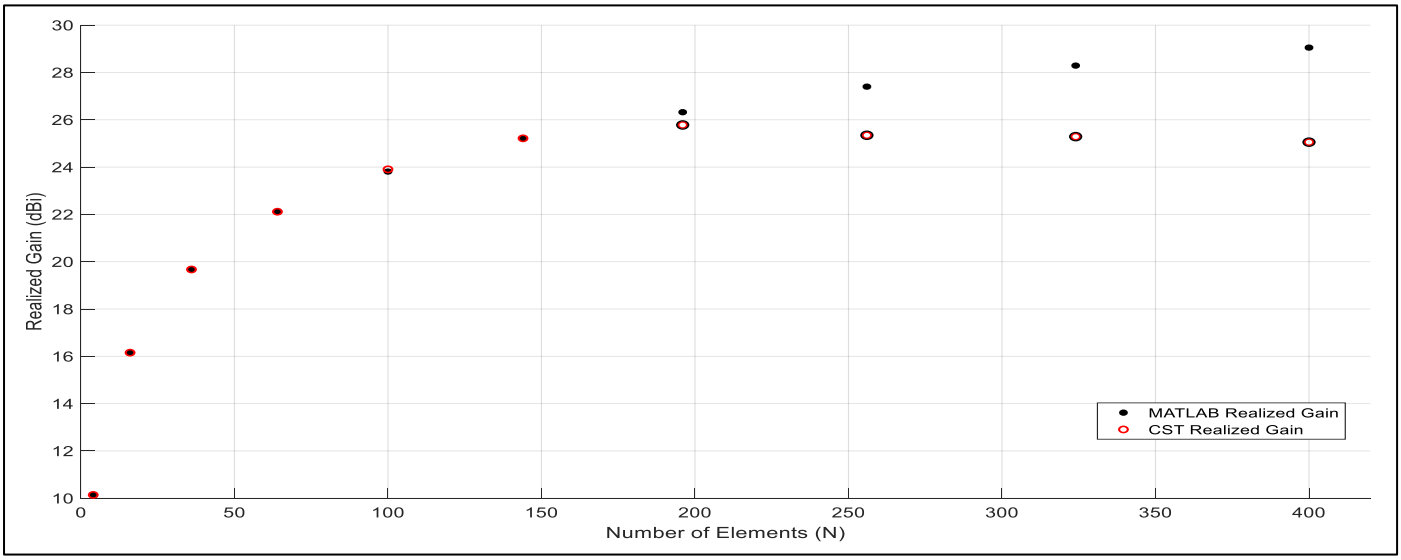

Fig 5 3D Radiation Directivity Plot (Representative Optimized Case).

ISSN No:-2456-2165 https://doi.org/10.38124/ijisrt/26jan461

Figure 6 contrasts the radiation patterns of the proposed super-directive design against a baseline configuration. It shows reduced sidelobe levels and improved beam shaping, validating the effectiveness of electromagnetic-aware excitation synthesis.

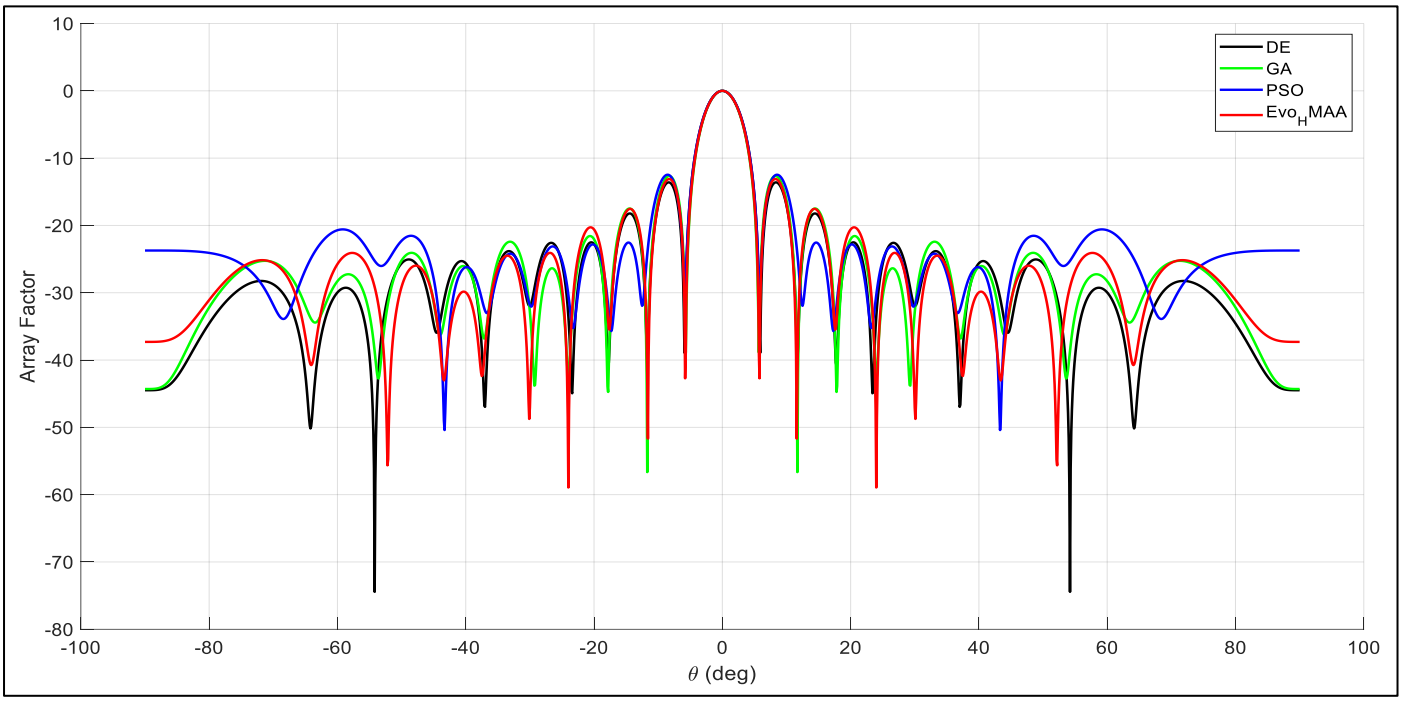

Fig 6 Radiation-Pattern Comparison for Evo-HMAA Versus Standard HMAA (10×10 Planar Array Case).

Figure 7 shows convergence behavior across optimization iterations, confirming stable and repeatable performance improvement. The absence of oscillatory or divergent behavior indicates robustness of the design methodology.

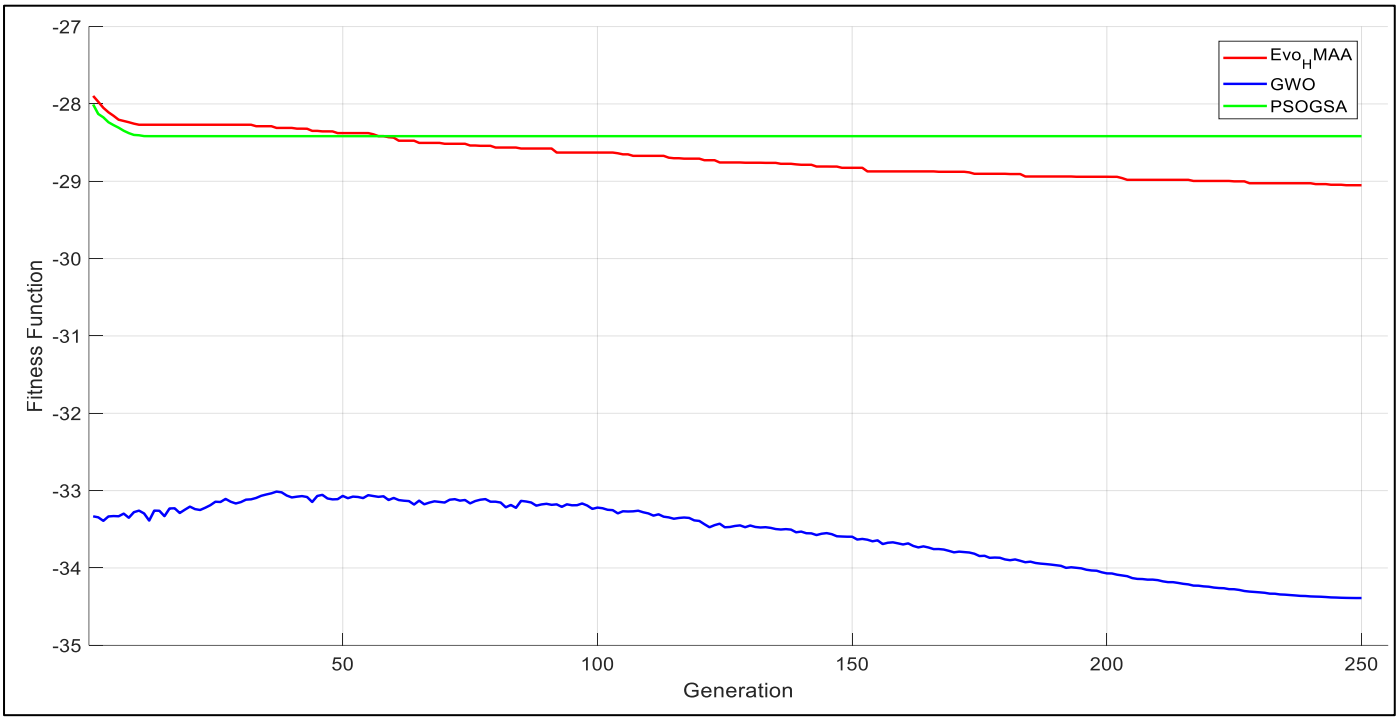

Fig 7 Convergence Comparison (10×10 Planar Array Case).

This figure demonstrates that optimized super-directive arrays maintain acceptable reflection coefficients despite aggressive excitation profiles. It directly addresses a major limitation of classical super-directivity by confirming practical impedance realizability.

ISSN No:-2456-2165 https://doi.org/10.38124/ijisrt/26jan461

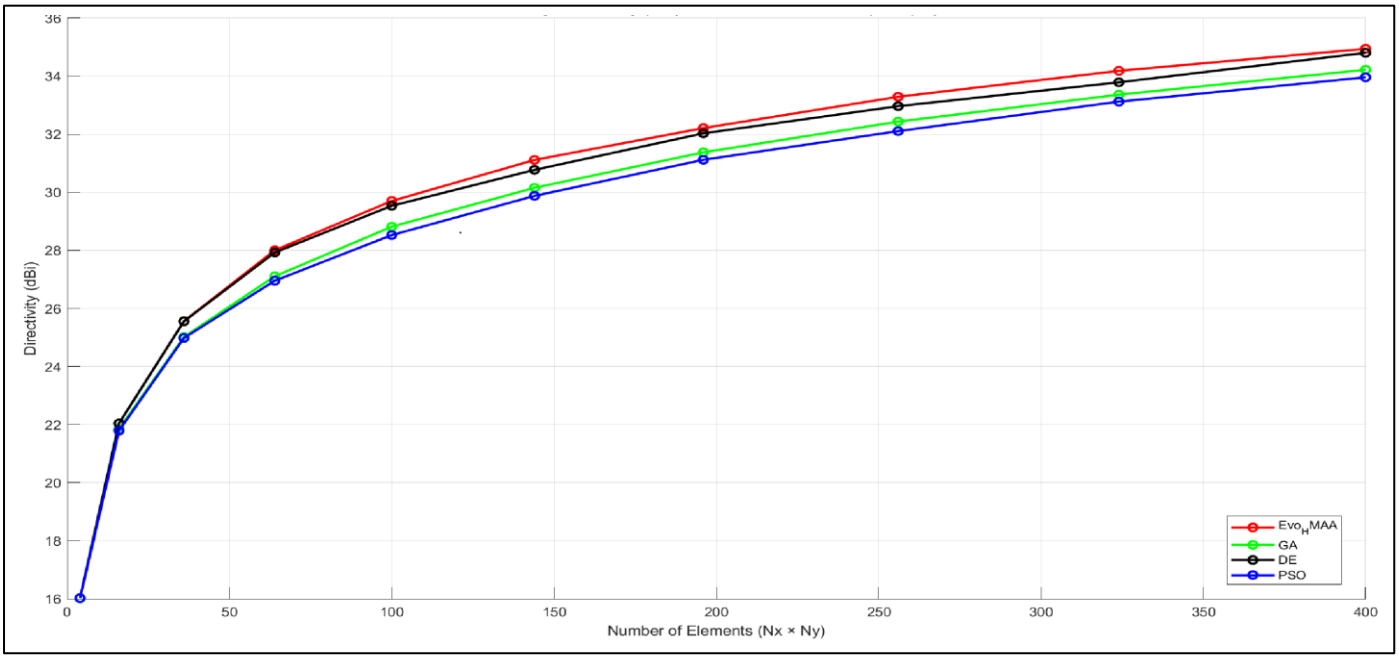

Fig 8 S11 Reflection-Coefficient Comparison for Evo-HMAA Versus Standard HMAA (10×10 Case).

To evaluate scalability, key performance metrics are extracted for HMIMO arrays of increasing size. Table 1 summarizes near-field directivity, focal intensity, sidelobe level, and efficiency for arrays ranging from 2×2 to 20×20 elements. The results demonstrate consistent performance improvements with increasing aperture size, validating the scalability of the proposed approach.

At the same time, diminishing returns are observed beyond certain array dimensions, where further increases in element count yield marginal gains relative to the associated increase in complexity and coupling. This behavior aligns with the physical bounds discussed in the literature and underscores the importance of balanced design choices.

Practical implementations of HMIMO arrays are subject to fabrication tolerances, component mismatches, and control errors. To assess robustness, small random perturbations are introduced into the optimized excitation amplitudes and phases

Figure 9 highlights the inverse relationship between directivity and sidelobe suppression. It reinforces the need for balanced design rather than single-objective optimization.

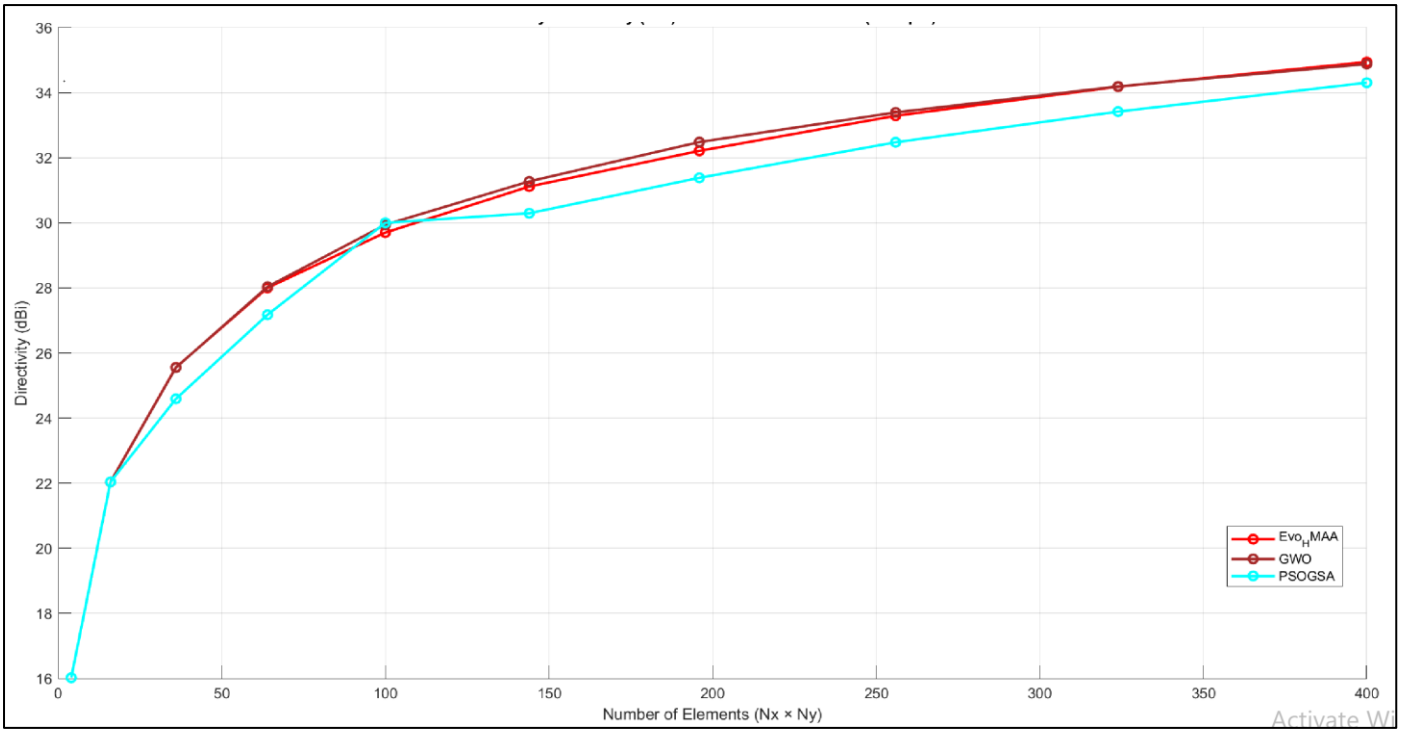

Fig 9 Array Directivity Versus Relative Sidelobe Level (SLL).

ISSN No:-2456-2165 https://doi.org/10.38124/ijisrt/26jan461

V. CONCLUSION

This paper investigated the electromagnetic realizability of near-field super-directive HMIMO arrays for 6G communications. By combining near-field theory with hard electromagnetic constraints and full-wave simulation validation, the study demonstrates that strong spatial focusing and improved sidelobe control are achievable without violating impedance and efficiency requirements, provided that the design process explicitly accounts for Q, matching, losses, and mutual coupling. The results support the viability of electromagnetically realizable super-directive HMIMO apertures for user-centric 6G links and sensing-centric applications. Future work should extend the framework toward wideband operation and hardware prototyping with measured validation.

REFERENCES

[1]. C. A. Balanis, Antenna Theory: Analysis and Design, 4th ed. Hoboken, NJ, USA: Wiley, 2016.
[2]. R. F. Harrington, “On the gain and beamwidth of directional antennas,” IRE Transactions on Antennas and Propagation, vol. 6, no. 3, pp. 219–225, Jul. 1958.
[3]. H. L. Thal, “New radiation Q limits for spherical wire antennas,” IEEE Transactions on Antennas and Propagation, vol. 54, no. 10, pp. 2757–2763, Oct. 2006.
[4]. L. J. Chu, “Physical limitations of omni-directional antennas,” Journal of Applied Physics, vol. 19, no. 12, pp. 1163–1175, Dec. 1948.
[5]. M. Gustafsson and S. Nordebo, “Bandwidth, Q factor, and resonance models of antennas,” Progress in Electromagnetics Research, vol. 62, pp. 1–20, 2006.
[6]. Poon, R. W. Brodersen, and D. N. C. Tse, “Degrees of freedom in multiple-antenna channels: A signal space approach,” IEEE Transactions on Information Theory, vol. 51, no. 2, pp. 523–536, Feb. 2005.
[7]. E. Björnson, L. Sanguinetti, and J. Hoydis, “Designing massive MIMO for beyond 5G,” IEEE Communications Magazine, vol. 57, no. 2, pp. 36–42, Feb. 2019.
[8]. S. Abadal et al., “Computing and communications for the software-defined metamaterial paradigm,” Nature Electronics, vol. 3, pp. 36–45, Jan. 2020.
[9]. Q. Wu and R. Zhang, “Towards smart and reconfigurable environment: Intelligent reflecting surface aided wireless network,” IEEE Communications Magazine, vol. 58, no. 1, pp. 106–112, Jan. 2020.
[10]. H. Yang, F. Gao, S. Jin, and C. Wen, “Near-field beamforming for extremely large-scale antenna arrays,” IEEE Communications Letters, vol. 25, no. 5, pp. 1525–1529, May 2021.
[11]. S. K. Sharma and D. S. Nagarkoti, “Meet the challenge of designing electrically small antennas,” *Microwaves & RF*, Aug. 19, 2017. [Online]. Available: https://www.mwrf.com/technologies/components/article/21848593/meet-the-challenge-of-designing-electrically-small-antennas
[12]. E. Demirors, G. C. Alexandropoulos, and M. Debbah, “Near-field communications for 6G: Fundamentals and opportunities,” IEEE Communications Magazine, vol. 60, no. 6, pp. 84–90, Jun. 2022.
[13]. M. Di Renzo et al., “Smart radio environments empowered by reconfigurable intelligent surfaces: How it works, state of research, and the road ahead,” IEEE Journal on Selected Areas in Communications, vol. 38, no. 11, pp. 2450–2525, Nov. 2020.
[14]. R. C. Hansen, Phased Array Antennas, 2nd ed. Hoboken, NJ, USA: Wiley, 2009.
[15]. R. F. Harrington and J. R. Mautz, “Theory of characteristic modes for conducting bodies,” IEEE Transactions on Antennas and Propagation, vol. 19, no. 5, pp. 622–628, Sep. 1971.
[16]. CST Studio Suite, “CST Microwave Studio – 3D EM Simulation Software,” Dassault Systèmes, 2023.
[17]. F. Molisch et al., “Hybrid beamforming for massive MIMO: A survey,” IEEE Communications Magazine, vol. 55, no. 9, pp. 134–141, Sep. 2017.
[18]. M. Z. Win et al., “Sensing and communication in the near field,” IEEE Communications Magazine, vol. 59, no. 6, pp. 84–90, Jun. 2021.
[19]. Y. Zeng, J. Xu, and R. Zhang, “Energy minimization for wireless communication with rotary-wing UAV,” IEEE Transactions on Wireless Communications, vol. 18, no. 4, pp. 2329–2345, Apr. 2019.